JOURNAL OF APPLIED POLYMER SCIENCE VOL. 21, 1813–1824 (1977)

Application of Rayleigh Spectroscopy to the Study of Emulsion and Dispersion Polymerization and Polymers

PAUL C. KILLGOAR, JR. and RAY A. DICKIE, *Engineering & Research Staff, Ford Motor Company, Dearborn, Michigan 48121*

Synopsis

Application of Rayleigh spectroscopy for characterization of particle size in nonaqueous dispersion and water-based emulsion paint resins is described. The technique allows a straightforward and rapid estimation of particle size; the measurement does not require exact determination of scatterer concentration. For monodisperse samples, unambiguous results are obtained for particles at least up to 50 μm in diameter; for polydisperse samples, an average size heavily weighted by large particles is obtained. Typical experimental results on monodisperse and polydisperse water-based latexes and on polydisperse nonaqueous dispersion resins are described. In the latter case, comparison of electron micrograph and light scattering size determinations indicates that the light scattering experiment yields approximately a z-average radius. Observations on particle formation and growth during polymerization are also described.

INTRODUCTION

Light scattering experiments—in contrast to electron microscope measurements, for example—allow particle size determinations to be made on polymer dispersions in virtually undisturbed condition. Classical techniques require the measurement of scattered intensity as a function of concentration and, usually, scattering angle. Extrapolation to zero concentration and scattering angle then yields a weight-average particle mass and a moment of the radius of gyration.[1] The availability of laser light sources and of sophisticated electronic signal processing equipment has made possible the development in recent years of new methods based on analysis of the frequency distribution of the scattered light. Extensive reviews of these techniques[2–5] and their application to the study of macromolecules in solution,[6,7] of biochemical systems,[8,9] and of aerosols[10] are available. Rayleigh spectroscopy, the technique discussed in this paper, is based on an analysis of the broadening of the spectral distribution of the (quasi) elastically scattered light. It allows determination of an average diffusion coefficient—and hence an average particle radius for spheres—with one light scattering measurement; at low concentrations, the measurement is independent of the number of scatterers present.

Rayleigh spectroscopy has been successfully applied to measurement of diffusion coefficients, molecular weights, and particle sizes. A study of intramolecular motion has also been reported.[11] Most of these studies have dealt with particles small with respect to the wavelength of light; many have been concerned with monodisperse systems. Measurements on larger particles have mostly been

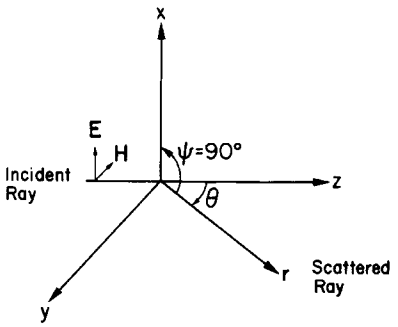

Fig. 1. Coordinate system for the light scattering experiment. Incoming monochromatic light is scattered from the origin. Spectrum of light scattered in the yz plane is determined at angle θ.

confined to monodisperse polystyrene latexes, the results being used to calibrate and define experimental procedures. In this paper, the application of Rayleigh spectroscopy to emulsion and dispersion polymerization and polymers, systems which are in general polydisperse and of relatively large size, is discussed. The determination and interpretation of an average particle size is discussed. Effects of size and polydispersity on experimental results are discussed qualitatively.

THEORY OF THE EXPERIMENT

The theory of quasi-elastic scattering has been treated extensively elsewhere[2–17] and will not be presented in detail here. Referring to Figure 1, an incident ray of monochromatic light polarized in the x direction is scattered from a point at the origin. The scattered light is observed in the zy plane at an angle θ. In practice, a laser is used as the source of the incident monochromatic radiation. The frequency shifts induced by particle diffusion are very small compared with the frequency of light and are essentially undetectable by conventional spectroscopic techniques. However, the spectrum of beat frequencies that is produced at the photocathode of a photomultipler by the interaction of light scattered from each particle with light scattered from every particle can be detected. Experimentally, the output of the photomultiplier is analyzed to obtain either the power spectrum of the photocurrent $S_i(\omega)$ or the current autocorrelation function $C_i(\tau)$. A complete discussion of the relationship between the intensity spectrum and its Fourier transform, the intensity autocorrelation function, and between these quantities and the experimentally determined functions discussed here can be found elsewhere.[3,4]

For monodisperse particles, $S_i(\omega)$ is a simple Lorentzian of half-width 2Γ:

$$S_i(\omega) = \frac{2\Gamma/\pi}{\omega^2 + 4\Gamma^2} \tag{1}$$

For particles undergoing Brownian diffusion, Γ is given by

$$\Gamma = D_T K^2 \tag{2}$$

where D_T is the translational diffusion coefficient and K is the scattering vector, a function of the scattering geometry:

$$K = \frac{4\pi n}{\lambda_0} \sin(\theta/2) \tag{3}$$

where λ_0 is the wavelength of the incident radiation *in vacuo* and n is the refractive index of the suspending medium. For spherical particles of radius R, D_T is assumed to be given by the Stokes–Einstein relationship

$$D_T = k_B T/6\pi\eta R \tag{4}$$

where k_B is Boltzmann's constant, T is the absolute temperature, and η is the viscosity of the suspending medium.

For polydisperse particles, $S_i(\omega)$ assumes a somewhat more complicated form:

$$S_i(\omega) = \frac{\sum_{j=1}^{n}\sum_{k=1}^{n} \Phi_j\Phi_k \dfrac{(\Gamma_j + \Gamma_k)/\pi}{\omega^2 + (\Gamma_j + \Gamma_k)^2}}{\sum_{j=1}^{n}\sum_{k=1}^{n} \Phi_j\Phi_k} \tag{5}$$

The factors Φ_i are time-independent scattered light intensities weighted for concentration. Thus, $S_i(\omega)$ for a polydisperse system is a weighted sum of Lorentzians.

The current autocorrelation function for monodisperse particles is given by (see, e.g., refs. 15, 16, and 18)

$$C_i(\tau) = \exp\left[-2\Gamma|\tau|\right] \tag{6}$$

while for a polydisperse system, $C_i(\tau)$ is given by

$$C_i(\tau) = \left\{\frac{\sum_{j=1}^{n} \Phi_j \exp\left[-\Gamma_j|\tau|\right]}{\sum_{j=1}^{n} \Phi_j}\right\}^2 \tag{7}$$

Analysis of experimental data for monodisperse systems can be handled in a straightforward manner by graphic or numerical techniques. Data on polydisperse systems present a more complicated problem. It has been shown that, with experimental data of sufficient accuracy, it is possible to extract characteristic moments of the diffusion coefficient distribution; alternatively, parameters characterizing an analytic distribution function can be obtained (see, e.g., refs. 7, 9, and 17–25).

Characterization of more than one or two parameters of a distribution requires data of considerable precision.[16–20,22] For rapid characterization of disperse systems, determination of an average size is often adequate. Since results on polydisperse systems can often be represented experimentally by a single exponential or Lorentzian, depending on the instrumentation used, a simplified analysis can be used to obtain an average value of the diffusion coefficient and hence of the particle size. The problem which remains is identifying the average obtained by the chosen method of data analysis.

The experimentally observed power spectrum is regarded as arising from a monodisperse system characterized by $\bar{\Gamma}$. The half-width of the power spectrum, $\omega_{1/2}$, is defined as the value of the frequency at which the power spectrum equals one half its value at zero frequency. The value of the power spectrum at $\omega_{1/2}$

is thus given by

$$S_i(\omega_{1/2}) = \frac{\sum_{j=1}^{n}\sum_{k=1}^{n} \frac{\Phi_j\Phi_k(\Gamma_j + \Gamma_k)/\pi}{\omega_{1/2}^2 + (\Gamma_j + \Gamma_k)^2}}{\sum_{j=1}^{n}\sum_{k=1}^{n} \Phi_j\Phi_k} \tag{8}$$

as well as by

$$\tfrac{1}{2}S_i(0) = \frac{\tfrac{1}{2}\sum_{j=1}^{n}\sum_{k=1}^{n} \frac{\Phi_j\Phi_k/\pi}{(\Gamma_j + \Gamma_k)}}{\sum_{j=1}^{n}\sum_{k=1}^{n} \Phi_j\Phi_k} \tag{9}$$

Combining these and letting $\omega_{1/2} = \bar{\Gamma}$, we obtain

$$\sum_{j=1}^{n}\sum_{k=1}^{n} \frac{\Phi_j\Phi_k[\bar{\Gamma}^2 - (\Gamma_j + \Gamma_k)^2]}{(\Gamma_j + \Gamma_k)[\bar{\Gamma}^2 + (\Gamma_j + \Gamma_k)^2]} = 0 \tag{10}$$

Unfortunately eq. (10) cannot be solved explicitly to obtain $\bar{R}$. For a sufficiently narrow distribution, however, it can be shown that $\bar{R}$ is approximately given by

$$\bar{R} = \left\{ \frac{\sum_{j=1}^{n}\sum_{k=1}^{n} \frac{\Phi_j\Phi_k R_jR_k}{(R_j + R_k)}}{\sum_{j=1}^{n}\sum_{k=1}^{n} \frac{\Phi_j\Phi_k(R_j + R_k)}{R_jR_k}} \right\}^{1/2} \tag{11}$$

The experimental results presented subsequently indicate that $\bar{R}$ determined in this way is close to, but somewhat higher than, that obtained by the current autocorrelation technique.

For the current autocorrelation function, the observed response is regarded as arising from a monodisperse system characterized by $\bar{\Gamma}$. Replacing Γ by $\bar{\Gamma}$ in eq. (6), setting the resulting expression for $C_i(\tau)$ equal to that given in eq. (7), we obtain

$$\exp[-\bar{\Gamma}|\tau|] = \frac{\sum_{j=1}^{n} \Phi_j \exp[-\Gamma_j|\tau|]}{\sum_{j=1}^{n} \Phi_j} \tag{12}$$

From eq. (12), by expansion of the exponentials and substitution from eqs. (2) and (4) and taking into account the fact that the function is evaluated at $\tau = 1/\bar{\Gamma}$,

$$\bar{R}_{(\tau=1/\bar{\Gamma})} = \frac{\sum_{j=1}^{n} \Phi_j \left\{1 - \frac{1}{2!}\left[1 - \left(\frac{\bar{R}}{R_j}\right)^2\right] + \frac{1}{3!}\left[1 - \left(\frac{\bar{R}}{R_j}\right)^3\right] - \cdots\right\}}{\sum_{j=1}^{n} \Phi_j/R_j} \tag{13}$$

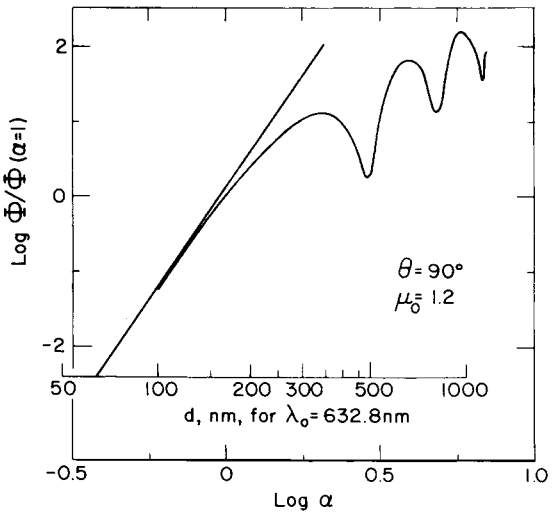

Fig. 2. Scattering function (reduced to unity at $\alpha = 1$) as a function of dimensionless parameter α for $\theta = 90°$, $\mu_0 = 1.2$; calculated from values tabulated in ref. 27.

The first term in the numerator expansion in eq. (13) yields

$$\bar{R} = \sum_{j=1}^{n} \Phi_j \Big/ \sum_{j=1}^{n} \Phi_j / R_j \tag{14}$$

The function Φ is proportional to the number of scatterers and, in addition, is a function of scattering angle θ, relative refractive index μ_0, wavelength λ_0, and particle size. The form of the scattering function is reviewed in detail in reference 26; extensive numerical tabulations are also available (see, e.g., ref. 27). Defining α as $2\pi R\mu_0/\lambda_0$, the function Φ_j assumes the form shown in Figure 2 (for $\theta = 90°$, $\mu_0 = 1.2$). For $\lambda_0 = 632.8$ nm, Φ_j is proportional to R^6 up to about 50 nm radius; eq. (14) becomes

$$\bar{R} = \sum_{j=1}^{n} N_j R_j{}^6 \Big/ \sum_{j=1}^{n} N_j R_j{}^5 \tag{15}$$

where N_j is the number of particles of radius R_j. The radius exponents are somewhat lower for larger particles, about 5 and 4 in numerator and denominator, respectively, up to radii of perhaps 100 to 125 nm. The first maximum in Φ_j occurs at α slightly over 2 ($\theta = 90°$). For polydisperse samples with a significant number of particles of large size, it may be advantageous to use smaller scattering angles θ for which the first maximum in Φ occurs at substantially larger values of α.

Systems with a sharply bimodal size distribution in which the constituent particle sizes differ substantially present at interesting special case. For the power spectrum, from eq. (5), if $R_1 \gg R_2$ and the concentrations are such that $\Phi_1 \gg \Phi_2$, it can readily be shown that

$$S_i(\omega) = \frac{2\Gamma_1/\pi}{\omega^2 + 4\Gamma_1{}^2} + \frac{2\Gamma_2/\pi}{\Phi_1(\omega^2 + \Gamma_2{}^2)} \tag{16}$$

Qualitatively, the power spectrum of eq. (16) comprises two Lorentzians—one, narrow and intense of half-width $2\Gamma_1$; the second, broader, less intense, and of

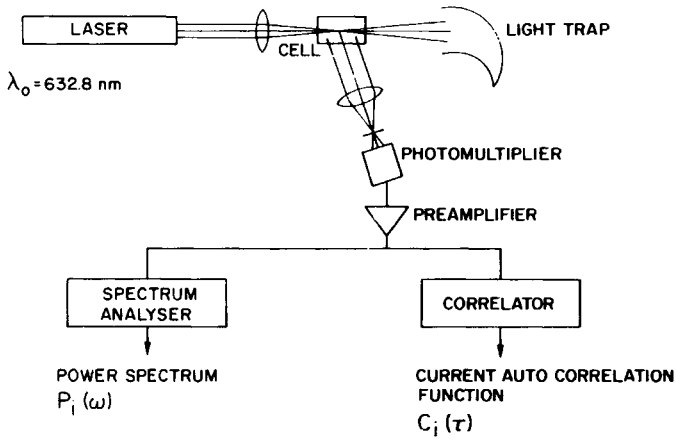

Fig. 3. Block diagram of light scattering apparatus described in text.

half-width Γ_2. For sufficiently large R_1/R_2, the expression degenerates into the form obtained for heterodyne detection—a Lorentzian of half-width Γ_2.

EXPERIMENTAL

The homodyne spectrometer is represented schematically in Figure 3. A 5-mW He–Ne laser of wavelength 632.8 nm is used as the monochromatic light source. A 250-mm focal length lens is used to focus the laser beam into the scattering cell. A quartz fluorescence cell is used as the sample cell. A second 250-mm focal length lens focuses the scattered light on a slit in front of the photomultiplier. The photomultiplier is an RCA 31034A phototube selected for its red sensitivity and linear frequency response. The photocurrent is amplified and then analyzed by either a Saicor 200-point real-time spectrum analyzer/averager or by a Saicor 100-point correlator. The final averaged spectrum or correlation function is displayed for visual inspection on an oscilloscope and read out digitally for subsequent computer manipulation.

With the experimental arrangement described, the practical lower limit of detection (for $\theta = 90°$) is about 70 nm with the He–Ne laser and about 20 nm with the He–Cd laser. As evident from the theoretical discussion, the practical upper limit of usage is a function of scattering angle, specimen polydispersity, and relative refractive index.

The spectrum analyzer and the correlator yield essentially the same information, albeit in somewhat different form. For monodisperse particles in the size range of interest here (20–500 nm) there is little compelling reason to choose one instrument over the other. For polydisperse samples, the correlator may be preferable; relative merits of the two techniques are discussed in reference 5.

Data have been analyzed by performing a nonlinear least-squares curve fitting routine[28] to eq. (1) or (6), as appropriate, to obtain Γ. DC and shot noise terms are treated as additional variables in the fitting procedure. For polydisperse systems, the method is used to obtain $\bar{\Gamma}$ for an equivalent monodisperse system.

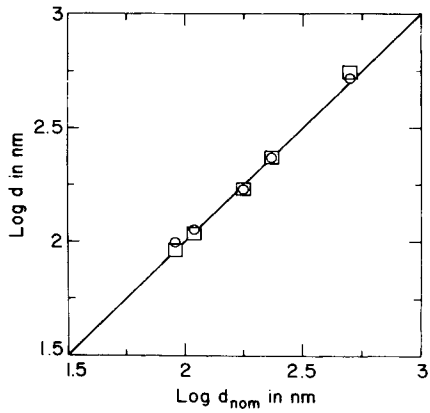

Fig. 4. Comparison of nominal (d_{nom}) and measured diameters (d) of monodisperse polystyrene latex spheres. Circles, spectrum analyzer determination; squares, correlator determination.

Illustrative light scattering experiments are reported here on three groups of materials: monodisperse polystyrene latexes and blends of monodisperse polystyrene latexes; acrylic copolymer latexes; and nonaqueous dispersions. The monodisperse polystyrene latexes were obtained from Dow Chemical Co. Acrylic copolymer latexes were synthesized by conventional procedures. Acrylic copolymer nonaqueous dispersions (NAD's) were supplied by Plastics, Paint, and Vinyl Operations of Ford Motor Company.

RESULTS

Monodisperse Polystyrene Spheres

Results on monodisperse latex spheres, presented in Figure 4, illustrate the correlation between particle diameter obtained by light scattering and that obtained by electron microscopic examination. A significant deviation is observed only for the largest particle size latex; this is thought to be due to the presence of some doublets (pairs of partly coalesced particles) in the specimen. Figure 4 also illustrates the excellent correlation between spectrum analyzer and correlator determinations of particle diameters for monodisperse spheres.

Blends of Monodisperse Spheres

The form of the equations for average radius for polydisperse spheres suggests that the quasi-elastic light scattering technique should be very sensitive to the presence of small numbers of large particles. This is illustrated by the results presented in Figure 5 on blends of monodisperse polystyrene latexes. (The experimental power spectra obtained showed some evidence of non-Lorentzian line shape, cf. eq. (16); in each case, however, a reasonably satisfactory representation in terms of a simple single Lorentzian could be obtained.)

For these blends, the presence of as little as one part per thousand of the larger particles was sufficient to significantly influence the average particle size obtained. Considerable care must be exercised in further interpretation of the data since one of the species present is relatively large ($\alpha > 1$). Thus, in Figure 5,

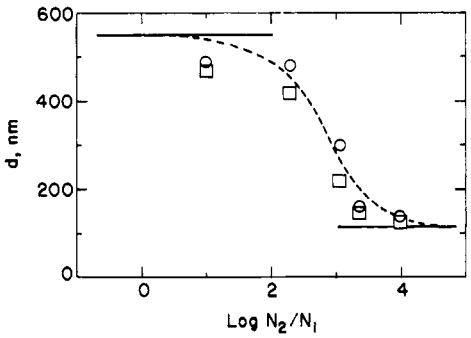

Fig. 5. Measured diameters of blends of monodisperse polystyrene latex spheres (d_1 = 550 nm, d_2 = 109 nm) as function of composition. Dashed curve calculated as

$$\overline{R} = \sum_{j=1}^{n} N_j R_j^5 \Big/ \sum_{j=1}^{n} N_j R_j^4.$$

results from both spectral and correlation function analysis are compared with a calculated average of the form

$$\overline{R} = \sum_{j=1}^{n} N_j R_j^5 \Big/ \sum_{j=1}^{n} N_j R_j^4 \tag{17}$$

Although the spectrum analysis results are somewhat higher than the correlation function figures, both sets agree fairly well with this (empirical) expression. Although this appears to be in gratifyingly close agreement with results predicted for correlation function analysis of moderately large particles, it must be regarded as an adventitious result: in these blends, Φ_j for the larger particles is somewhat beyond its first minimum, and no broad significance can be attached to the form of radius average shown.

Nonaqueous Dispersion Polymerization

Quasi-elastic light scattering is particularly well suited to the monitoring of particle formation and growth in disperse polymer systems since measurements can be completed relatively quickly and concentrations need not be known accurately. This application is illustrated first by measurements of particle size of nonaqueous dispersion systems as a function of polymerization time. Results for two different systems are illustrated in Figure 6. The initial negative slope indicates that a population of relatively large particles is formed in the first stage of polymerization; as the polymerization proceeds, average particle size drops significantly. From the form of eqs. (11) and (13), and from the data presented in the preceding section on latex blends, it appears likely that large particles must be few in number and formed primarily at the beginning of the polymerization. The slow increase in particle diameter at long polymerization times probably represents a combination of particle growth through polymerization of residual monomer and possibly through particle coalescence.

Electron-microscopic examination of finished nonaqueous dispersions reveals a very broad distribution including a small proportion of very large particles. These results are summarized in Figure 7 for four samples that have similar number-average particle size. Number, mass, and z-average sizes computed from the data of Figure 7 are compared in Table I with light scattering results.

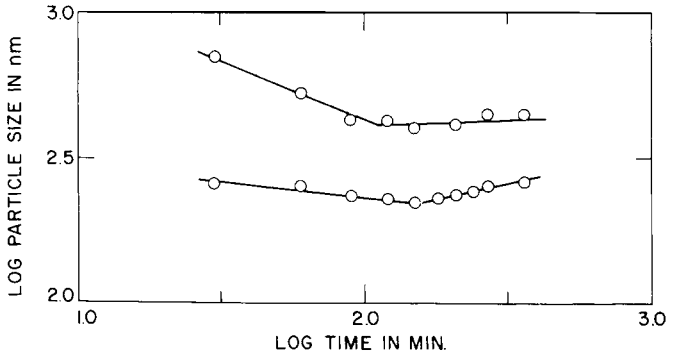

Fig. 6. Particle size as function of polymerization time for two nonaqueous dispersion polymerizations.

(The number average of property P is $\bar{P}_n = \Sigma N_j P_j / \Sigma N_j$; the mass average is $\bar{P}_m = \Sigma N_j M_j P_j / \Sigma N_j M_j$; the z average is $\bar{P}_z = \Sigma N_j M_j^2 P_j / \Sigma N_j M_j^2$. For spherical particles, the average radii are given by $\bar{R}_n = \Sigma N_j R_j / \Sigma N_j$; $\bar{R}_m = \Sigma N_j R_j^4 / \Sigma N_j R_j^3$; and $\bar{R}_z = \Sigma N_j R_j^7 / \Sigma N_j R_j^6$. Many other averages could be calculated—see, e.g., ref. 29—but the differences in numerical values of the higher averages are rather small.) The data of Figure 7 characterize the number distribution of particles fairly well. The higher calculated moments are not very reliable, however, as they are dominated by single particle counts at the high end of the size distribution. Comparison of average size as determined by light scattering with calculated averages, thus does not allow an unambiguous identification of the light scattering average. The results do indicate that the light scattering average is a high average, approximating a z average in three of the examples shown.

A further problem in characterization of the average of particle size arises because of the relatively large size of the particles. The average obtained depends on details of the size distribution through the scattering function Φ_j. Since the size distribution is broad and continuous, however, the effect of the oscilla-

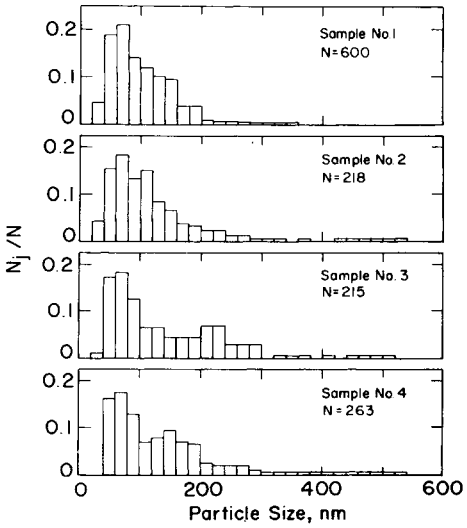

Fig. 7. Normalized histograms showing distribution of particle size for four nonaqueous dispersion samples of approximately the same number-average size.

TABLE I
Comparison of Light Scattering and Electron Micrograph Particle Size Determinations for Nonaqueous Dispersion Samples

Type of average	Particle size, nm, for sample number			
	1	2	3	4
Number average	100	103	136	130
Mass average	194	354	309	360
z Average	285	472	428	478
Light scattering measurement	287	436	477	340

tions in Φ_j will tend to be smoothed out somewhat. The average obtained cannot be defined in simple terms—e.g., as a z average—even though it may be reproducible and characteristic of the sample.

For the nonaqueous dispersions discussed thus far, power spectra could be represented satisfactorily as single Lorentzians. Figure 8 illustrates a single exception which could not be so treated. Electron-microscopic examination of this sample reveals a sharply bimodal distribution comprising a small number of particles between about 300 and 400 nm in diameter and a much larger number between about 40 and 80 nm in diameter (the number ratio could not be accurately determined). A qualitative decomposition of the power spectrum into two Lorentzians, consistent with eq. (16), is shown. This decomposition indicates a size ratio of about 4 and a number ratio of about 1/2000.

Emulsion Polymerization

Particle formation and growth in conventional emulsion polymerization can also be monitored conveniently by quasi-elastic light scattering. Since the particle sizes are often smaller in emulsion polymerization than in nonaqueous dispersion polymerization, and since the size distributions are usually narrower, the average size obtained is better defined and closer to that provided by microscopic techniques. Results for three polymerizations are summarized in Figures 9 and 10. In each polymerization, monomers were added throughout the first 2.5 hr of reaction time. The polymerizations differed only in choice and

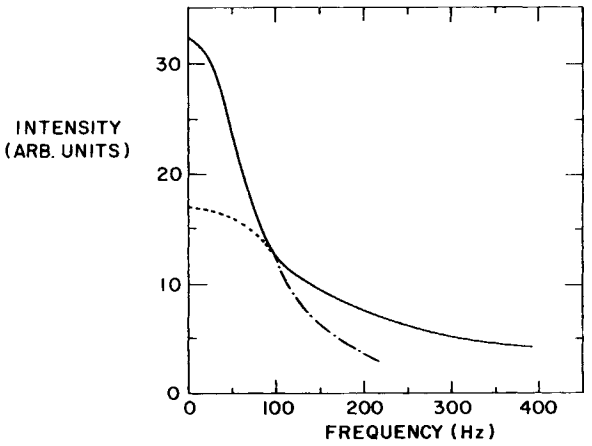

Fig. 8. Power spectrum for a sharply bimodal nonaqueous dispersion. A qualitative decomposition according to eq. (16) is shown.

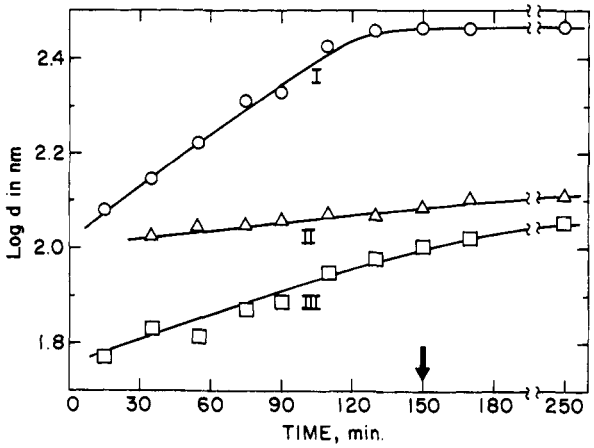

Fig. 9. Particle size as function of polymerization time for three emulsion polymerizations. Arrow indicates end of monomer addition. Numbers label curves for identification in text.

method of employment of surfactants. The end of monomer addition is indicated in each figure by an arrow on the time axis. In each case, average particle size increases (see Fig. 9), consistent with at least some growth of particles formed early in the reaction. Dividing the total volume of monomer by the volume of an average particle (as calculated from the average diameter) gives a measure of the total number of particles present. These results, plotted in Figure 10, indicate that for polymerization I, virtually all monomer added after the first 20 to 30 min of reaction polymerizes within existing particles; for polymerization II, the number of particles increases steadily throughout the addition of monomer; for polymerization III, the number of particles begins to decrease part-way through the reaction period: this is most likely indicative of particle coalescence. The latex from polymerization III did, in fact, display a substantial quantity of coagulum at the end of polymerization.

Measurements of particle size by quasi-elastic light scattering have also been used in this laboratory to assess effects of changes in pH, solvent composition, and ionic strength on polymer latexes. In principle, measurements by the quasi-elastic method can be combined with turbidity measurements to obtain both size and concentration of scatterers independent of gravimetric solids de-

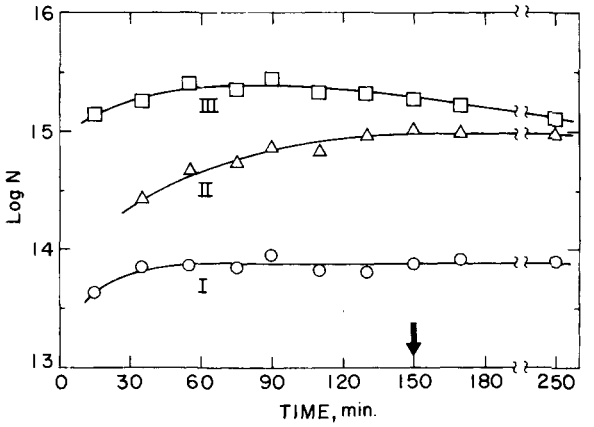

Fig. 10. Total number of particles as function of time for polymerizations of Fig. 9. Key as for Fig. 9.

terminations, providing a powerful tool for characterization of disperse systems.

CONCLUDING REMARKS

Quasi-elastic light scattering is a convenient means of determining average particle size in typical paint resin dispersions, particularly when the concentration of scatterers is difficult to determine. For monodisperse spheres, the technique can give unambiguous answers for even quite large particles. For polydisperse systems, some caution is necessary in choice of scattering angle and in interpretation of results, but qualitatively useful information is readily obtained.

The assistance of colleagues is gratefully acknowledged. Mrs. B. Bergman performed many of the light scattering measurements; H. K. Plummer, the electron microscopic analysis of particle size. J. D. Nordstrom provided the nonaqueous dispersion samples. L. Rimai, I. Salmeen, and H. vanOene offered many helpful suggestions.

References

1. C. Tanford, *Physical Chemistry of Macromolecules,* Wiley, New York, 1961, Chap. 5.
2. B. Chu, *Ann. Rev. Phys. Chem.*, **21,** 145 (1970).
3. W. L. Peticolas, *Advan. Polym. Sci.*, **9,** 285 (1972).
4. B. Chu, *Laser Light Scattering,* Academic Press, New York, 1974.
5. H. Z. Cummins, in *Photon Correlation and Light Beating Spectroscopy,* H. Z. Cummins and E. R. Pike, Eds., Plenum Press, New York, 1973.
6. R. J. Blagrove, *J. Macromol. Sci.*, **C9,** 71 (1973).
7. P. N. Pusey, in *Photon Correlation and Light Beating Spectroscopy,* H. Z. Cummins and E. R. Pike, Eds., Plenum Press, New York, 1973.
8. N. C. Ford, Jr., *Chem. Scrip.*, **2,** 193 (1972).
9. H. Z. Cummins, in *Photon Correlation and Light Beating Spectroscopy,* H. Z. Cummins and E. R. Pike, Eds., Plenum Press, New York, 1973.
10. W. C. Hinds and P. C. Reist, *J. Aerosol Sci.*, **3,** 501 and 515 (1972).
11. W-N. Huang and J. E. Frederick, *Macromolecules,* **7,** 34 (1974).
12. R. Pecora, *J. Chem. Phys.*, **40,** 1604 (1964).
13. Y. Tagami and R. Pecora, *J. Chem. Phys.*, **51,** 3293 (1969).
14. N. A. Clark, J. H. Lunacek, and G. B. Benedek, *Amer. J. Phys.*, **38,** 575 (1970).
15. D. E. Koppel, *J. Appl. Phys.*, **42,** 3216 (1971).
16. D. E. Koppel, *J. Chem. Phys.*, **57,** 4814 (1972).
17. D. S. Thompson, *J. Chem. Phys.*, **54,** 1411 (1971); *J. Phys. Chem.*, **75,** 789 (1971).
18. J. C. Brown, P. N. Pusey, and R. Dietz, *J. Chem. Phys.*, **62,** 1136 (1975).
19. C. R. Bargeron, *J. Chem. Phys.*, **61,** 2134 (1974).
20. F. C. Chen, W. Tscharmuter, D. Schmidt, and B. Chu, *J. Chem. Phys.*, **60,** 1675 (1974).
21. P. N. Pusey, D. E. Koppel, D. W. Schaefer, R. D. Camerini-Otero, and S. H. Koenig, *Biochemistry,* **13,** 952 (1974).
22. C. B. Bargeron, *J. Chem. Phys.*, **60,** 2516 (1974).
23. C. B. Bargeron, *Appl. Phys. Lett.*, **23,** 379 (1973).
24. T. Tanaka, *Polym. J.*, **7,** 62 (1975).
25. S. P. Lee and B. Chu, *Appl. Phys. Lett.*, **24,** 261 (1974).
26. M. Kerker, *The Scattering of Light and Other Electromagnetic Radiation,* Academic Press, New York, 1969.
27. W. J. Pangonis and W. Heller, *Angular Scattering Functions for Spherical Particles,* Wayne State University Press, Detroit, 1960.
28. J. L. Dye and V. A. Nicely, *J. Chem. Educ.*, **48,** 443 (1971).
29. H.-G. Elias, R. Bareiss, and J. G. Watterson, *Advan. Polym. Sci.*, **11,** 111 (1973).

Received April 12, 1976
Revised May 17, 1976